JOURNAL OF MATERIALS SCIENCE 32 (1997) 5725–5736

# Microscopic examination of the microstructure and deformation of conventional and auxetic foams

N. CHAN
*Institute of Aeronautics and Astronautics, National Cheng Kung University, Tainan, Taiwan 70101*

K. E. EVANS
*School of Engineering, Harrison Engineering Building, The University of Exeter, Exeter EX4 4QF, UK*

Auxetic materials have a negative Poisson's ratio, that is, they expand laterally when stretched longitudinally. One way of obtaining a negative Poisson's ratio is by using a re-entrant cell structure. Auxetic foam was fabricated from a conventional polymeric foam. Assuming similar mechanical properties for the solid material comprising the foams, the principle variable affecting the properties of the foam is the geometry of the cells. This means that the unusual mechanical properties of auxetic foams are attributed to the deformation characteristics of re-entrant microstructures. In this paper, the results of optical- and scanning electron-microscopic studies of the geometrical parameters for the different foams examined are presented. Examples of the microstructural deformation mechanisms observed are also presented. Comparison between the conventional foams and their auxetic conversions are also made.

## 1. Introduction

Foams have found a wide range of applications. Their unusual mechanical properties arise from their porous cellular structure. In theory, there are two ways of improving the mechanical properties of conventional foams: (i) by altering the chemical constituents of the solid struts or (ii) by changing the cell geometry. Much of the work performed in this area has concentrated on changing the chemical composition of the foam. Most recently, attempts have been made to look for a new way to improve the mechanical properties based on changing the foam cell geometry.

In 1987, a very interesting new type of foam was developed by Lakes [1]. This polymeric foam had a Poisson's ratio of $-0.7$. Although it was generally believed that all materials have a positive Poisson's ratio, it has been accepted that a negative Poisson's ratio, is theoretically possible [2]. One way of obtaining a negative Poisson's ratio is by using a re-entrant cell structure [3]. In addition to this early work several other examples of materials with a negative Poisson's ratio have been reported [4–6] and the term "auxetic materials" has been introduced [7] to describe this group of materials.

At first sight, one might suppose that the mechanical properties of a foam would depend significantly on cell size. However, it is known that cell size makes only a minor contribution. A much more significant contribution is attributed to the cell shape [8]. When the cells are equiaxed the properties are isotropic, but when the cells become slightly elongated or flattened then the properties will depend on direction, often to a significant extent. Three dimensional foams, in which the cell walls have random orientations in space, are normally anisotropic, which is due to the way they are foamed. A cellular foam is produced by dispersing the gas within a semi-liquid solid material which is allowed to solidify whilst the gas bubbles are still present. The direction in which the bubbles rise through the semi-liquid phase is known as the rise direction. Usually, the bubbles elongate as they rise in the solidified foam and often the bubble shape is different in the rise and transverse directions. This effect can lead to an isotropic behaviour. Assuming similar mechanical properties for the solid material comprising the foams, the principle variable affecting the properties of the foam is the geometry of the cells.

There are three different types of foam cell structure: open-cell, closed-cell and reticulated foams. The distinctions between these three foams are that closed-cell foams have a membrane of variable thickness covering each face of the cell. In an open cell foam, most of these membranes are perforated, and in reticulated foams the membranes have all been removed by chemical means or with the help of a heat treatment. These foams can be used as filters. In practice,

0022–2461  

these cellular morphologies can co-exist so that a polymer foam is not always completely open or closed.

In the majority of cases examined here the foams used were reticulated. In order to clarify the deformation mechanisms in the foam, a thinning method was developed to vary the rib thickness of the foam. This also enabled us to examine the variation in modulus with rib thickness.

A relatively simple conversion process may be used to convert conventional reticulated foams into auxetic foams. This process is described in detail elsewhere [11]. In this paper the results of optical and scanning electron microscope studies of the geometrical parameters for the different foams examined are presented. Examples of the microstructural deformation mechanisms observed are also presented.

In the next section the experimental methods are described, followed by a section showing the microstructures and deformation mechanisms seen, with a comparison between conventional and auxetic foams. The results for rib thinning are also presented. This is followed by the interpretation and discussion of the results obtained.

## 2. Experimental procedures

### 2.1. Fabricating auxetic foams

One way of obtaining a negative Poisson's ratio is by using a re-entrant cell structure. Various features of the re-entrant cell shape can be controlled by processing techniques. The method used for the manufacture of auxetic samples involved four stages: (i) compression, (ii) heating, (iii) cooling and (iv) relaxation [1]. To transform a conventional flexible foam [9] into an auxetic one using this method requires that the foam is simultaneously compressed in three dimensions to force the cell ribs to buckle. This produces a re-entrant structure which is then heated to its softening temperature to preserve the new configuration. Different types of polymeric foam (e.g., open or reticulated) and different densities of conventional foams require different heating times and temperatures. More details on the fabrication of the auxetic foams used here can be found elsewhere [10, 11].

### 2.2. Thinning down the cell rib thickness

A further method available to vary the cell geometry is to alter the cell rib thickness to length ratio. A method has been developed to vary the rib thickness.

This was effected by the use of a water bath containing a 10% solution of sodium hydroxide (NaOH) in water. Specimens were cut to dimensions of: $25 \times 25 \times 140$ mm with an average error of $\pm 1$ mm using a Burgess band saw. The temperature of the water bath was kept at 50 °C. First, a number of specimens were put into the sodium hydroxide solution using tongs, and a thin perforated stainless steel plate was used to hold them in position below the surface of the solution. Every 5 min a specimen was taken out of the water bath and then washed using clean water for 30 min at room temperature. Finally, all of the thinned foams were left to dry at room temperature for 1 day. To examine any effect on the mechanical properties of the foam, the tensile modulus was measured. Specimens with different rib thickness were prepared as described earlier. The tensile tests were carried out using an Instron 4505 instrument at a crosshead speed of 2 mm $min^{-1}$. Four specimens were tested in each case.

### 2.3. Examining the microstructures of foams

Polymeric foams have been examined using both optical and scanning electron microscopy (SEM). Each foam sample was sectioned into one of the three dimensions using a Burgess band saw, and then photographs were taken of each sample. The specimens prepared for SEM examination were coated with gold using an Edwards Sputter Coater S150, and examined with a Philips 501 SEM. Photographs were taken during the scanning process. From these micrographs, estimates of the important geometric parameters for analysis of the mechanical properties were obtained. These parameters are the cell rib thickness, cell rib length, and cell shape.

The microstructure of the foam is very complicated. To characterize the cell geometry of the foam, we need some way of averaging the cell geometry. To do this the foam in question was encapsulated in a resin matrix (Scandiplast 9101 resin). This was subsequently sectioned and polished, using standard metallographic methods. Fig. 1 is a photograph of such a section and shows that each conventional foam cell is approximately represented by an ellipsoid. Using this method it is possible to define the specific planes perpendicular and parallel to the rise direction. Thus the mean dimensions of the cells in the rise and transverse directions could be obtained by measurement from photographs such as that shown as Fig. 1. The parameters required were those needed to relate the microstructure of the real foams to that of the model structures shown in Fig. 2(a and b). These models are described is detail elsewhere [11], but, basically, the cell geometry chosen is one that meets the main requirements of three dimensional anisotropy and one that is readily convertible from a conventional to an

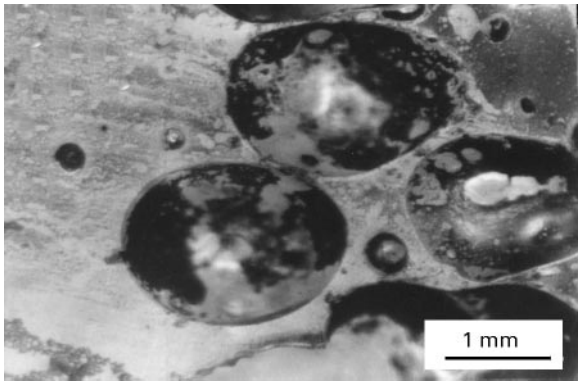


*Figure 1* Looking at the 60 p.p.i. reticulated polyester urethane foam (PECO) along the *x* axis (Face A). (Optical microscopy). This was done by using Scandiplast 9101 resin to fill the foam specimen and grinding the faces plane-parallel after hardening.

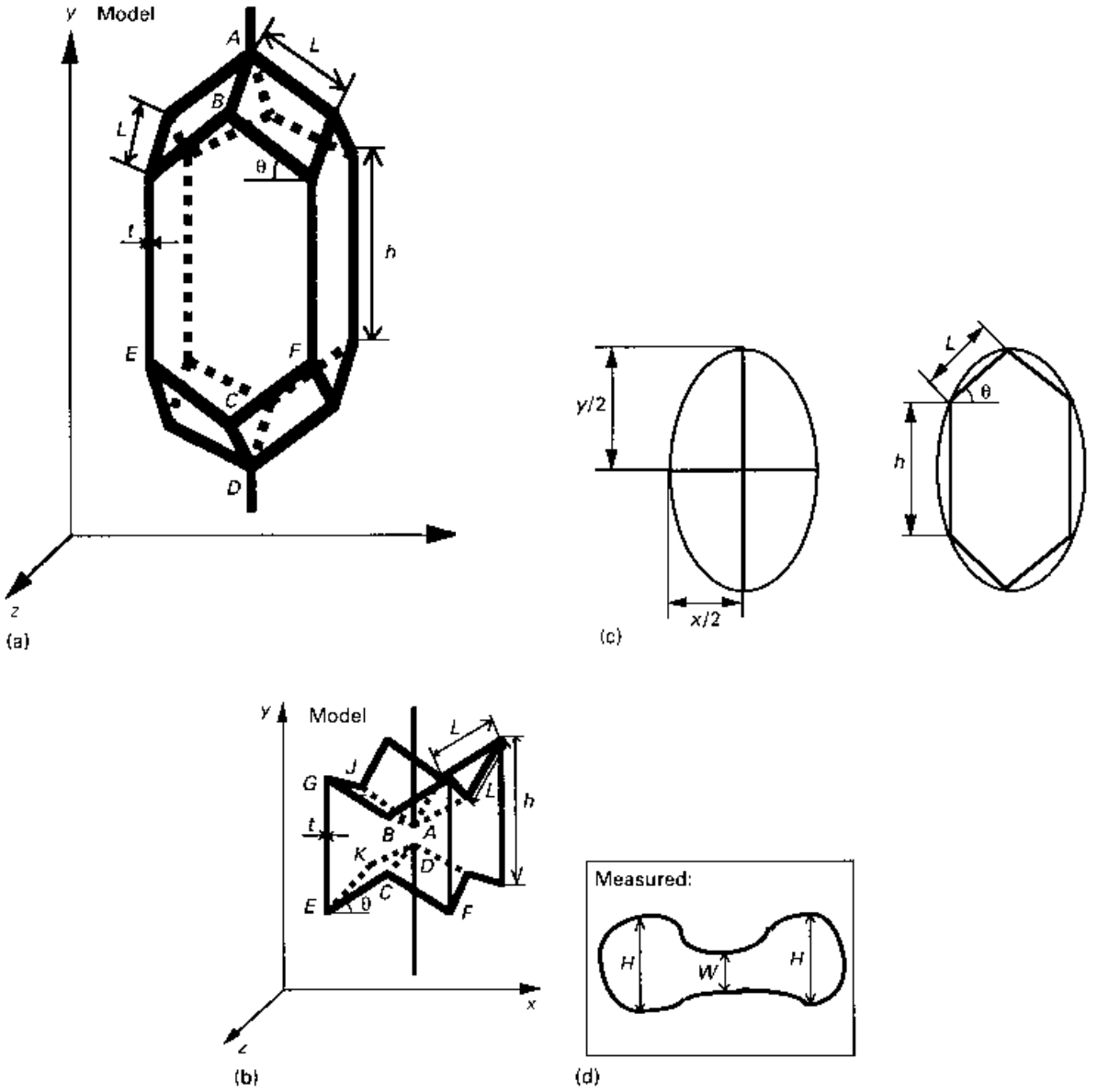


*Figure 2* A schematic representation of the cell geometric parameters of a foam. (a) A model of conventional foam cell. The length of the cell rib along the foam rise direction is $h$, the length of the cell rib in the other directions is $L$. The cell angle is θ. (b) A model of an auxetic foam cell and (c) a schematic diagram of a conventional foam cell. θ is positive for both auxetic and conventional foams (d) a schematic diagram of a re-entrant foam cell.

auxetic foam structure. The data from these specimens was then related to the model parameters as follows. For a conventional cell (Fig. 2a) the maximum cell length $AD$ is given by:

$$AD = h + 4L\sin\theta \quad (1)$$

The minimum cell length $BC$ is given by:

$$BC = h + 2L\sin\theta \quad (2)$$

Hence the average cell height, equivalent to the mean dimension of the ellipsoids in the foam rise direction is:

$$y = h + 3L\sin\theta \quad (3)$$

Similarly, the width of the cell $EF$ is given by

$$EF = 2L\cos\theta \quad (4)$$

This is equivalent to the mean width of the ellipsoids in both the $x$ and $y$ directions. Hence,

$$x = 2L\cos\theta \quad (5)$$

For the same foam, after conversion to an auxetic foam we have:

$$EF = 2L\cos\theta \quad (6)$$

Whereas now the minimum height, $BC$ is given by

$$BC = h - 2L\sin\theta \quad (7)$$

While the maximum height, $GE$ is given by

$$GE = h \quad (8)$$

Hence the average height of the cell, $H$, is:

$$H = h - L\sin\theta \quad (9)$$

Similarly the maximum, mid-plane waist height, $JK$, is:

$$JK = h - 2L\sin\theta \quad (10)$$

and the minimum, $AD$, is:

$$AD = h - 4L\sin\theta \quad (11)$$

Hence the average mid-plane waist length, $W$, is:

$$W = h - 3L\sin\theta \quad (12)$$

The data, $x$, $y$, $H$ and $W$ were obtained from the measurements of about 100 cells in each direction for each foam specimen. Equations 9 and 12 combined with Equations 3 and 5 for the same foam in the non-auxetic state gives all the parameters necessary for the geometric model of the cell. Examples for measuring the concave cells and convex cells are shown in Fig. 2(c and d).

### 2.4. Observation of microstructural deformation mechanisms

The microstructural deformation behaviour of the individual cells of the foam were studied using Wild M8 and MPS45 optical microscopes for different modes of loading, i.e., tension, compression and shear, using small specimens (dimensions, $40 \times 10 \times 5$ mm). The investigations described here were performed on the previously described conventional and auxetic PUR flexible foams. Various foam densities, cell sizes and cell shapes were studied. A vice was used to deform the samples under the optical microscope.

## 3. Results

### 3.1. The microstructure of conventional foam

The classical example of a low density foam is the reticulated PU (polyurethane) foam, and micrographs for this type of material have been presented many times in the literature [8–10, 12]. The conventional foams used in this work are listed in Tables I to V, with the geometric parameters obtained as described in Section 2.3. An example is presented in Fig. 3(a–c). It is seen that the 60 p.p.i. (pores per inch) polyester urethane foam consist of interconnecting struts; close examination indicated that the predominant configuration is an array of cells with pentagonal faces. The foam is an anisotropic material since, as previously explained, when observed from above the cells are more circular and smaller in the foam rise direction than that in the other two directions.

TABLE I Characterization data for the 60 p.p.i. reticulated conventional polyester urethane foam (short hand: PECO)

| Material | Flexible polyester urethane (PECO) |
|---|---|
| Density, ρ ($kg\,m^{-3}$) | $33.7 \pm 1.3$ |
| Open or closed cells | Reticulated |
| Mean edges per face | $5 \pm 1$ |
| Mean faces per cell | $12 \pm 2$ |
| Symmetry of structure | Axisymmetry |
| Mean cell edge thickness, $t$ (mm) | $0.087 \pm 0.025$ |
| Average height of cell, (mm) | $2.53 \pm 0.21$ |
| Average width of cell, (mm) | $1.92 \pm 0.16$ |
| Rib length along the foam rise direction, $h$ (mm) | $1.30 \pm 0.044$ |
| Rib length along the other directions, $L$ (mm) | $0.58 \pm 0.022$ |
| Cell angle, θ (deg) | $32 \pm 2.2$ |

TABLE II Characterization data for the 60 p.p.i. closed-cell conventional polyester urethane foam (short hand: PECC)

| Material | Flexible polyester urethane (PECC) |
|---|---|
| Density, ρ ($kg\,m^{-3}$) | $37.9 \pm 2.1$ |
| Open or closed cells | Closed |
| Mean edges per face | $5 \pm 1$ |
| Mean faces per cell | $12 \pm 2$ |
| Symmetry of structure | Axisymmetry |
| Mean cell edge thickness, $t_f$ (mm) | $0.002 \pm 0.001$ |
| Mean cell edge thickness, $t$ (mm) | $0.045 \pm 0.018$ |
| Average height of cell, (mm) | $1.08 \pm 0.15$ |
| Average width of cell, (mm) | $0.47 \pm 0.08$ |
| Rib length along the foam rise direction, $h$ (mm) | $0.67 \pm 0.011$ |
| Rib length along the other directions, $L$ (mm) | $0.27 \pm 0.005$ |
| Cell angle, θ (deg) | $30 \pm 2.6$ |

TABLE III Characterization data for the 10 p.p.i. open-cell conventional polyether urethane foam (short hand: 10CO)

| Material | Flexible polyether urethane (10CO) |
|---|---|
| Density, ρ ($kg\,m^{-3}$) | $24.1 \pm 3.1$ |
| Open or closed cells | Open cells |
| Mean edges per face | $5 \pm 1$ |
| Mean faces per cell | $12 \pm 2$ |
| Symmetry of structure | Axisymmetry |
| Mean cell edge thickness, $t$ (mm) | $0.23 \pm 0.015$ |
| Average height of cell, (mm) | $4.93 \pm 0.27$ |
| Average width of cell, (mm) | $2.57 \pm 0.19$ |
| Rib length along the foam rise direction, $h$ (mm) | $2.33 \pm 0.047$ |
| Rib length along the other directions, $L$ (mm) | $1.55 \pm 0.021$ |
| Cell angle, θ (deg) | $34 \pm 3.0$ |

TABLE IV Characterization data for the 30 p.p.i. open-cell conventional polyether urethane foam (short hand: 30CO)

| Material | Flexible polyether urethane (30CO) |
|---|---|
| Density, ρ ($kg\,m^{-3}$) | $24.5 \pm 2.7$ |
| Open or closed cells | Open cells |
| Mean edges per face | $5 \pm 1$ |
| Mean faces per cell | $12 \pm 2$ |
| Symmetry of structure | Axisymmetry |
| Mean cell edge thickness, $t$ (mm) | $0.13 \pm 0.025$ |
| Average height of cell, (mm) | $3.18 \pm 0.25$ |
| Average width of cell, (mm) | $1.47 \pm 0.16$ |
| Rib length along the foam rise direction, $h$ (mm) | $1.80 \pm 0.044$ |
| Rib length along the other directions, $L$ (mm) | $0.87 \pm 0.022$ |
| Mean cell angle, θ (deg) | $32 \pm 2.0$ |

TABLE V Characterization data for the 60 p.p.i. open-cell conventional polyether urethane foam (short hand: 60CO)

| Material | Flexible polyether urethane (60CO) |
|---|---|
| Density, ρ ($kg\,m^{-3}$) | $21.7 \pm 1.9$ |
| Open or closed cells | Open cells |
| Mean edges per face | $5 \pm 1$ |
| Mean faces per cell | $12 \pm 2$ |
| Symmetry of structure | Axisymmetry |
| Mean cell edge thickness, $t$ (mm) | $0.036 \pm 0.002$ |
| Average height of cell, (mm) | $0.65 \pm 0.11$ |
| Average width of cell, (mm) | $0.34 \pm 0.07$ |
| Rib length along the foam rise direction, $h$ (mm) | $0.38 \pm 0.018$ |
| Rib length along the other directions, $L$ (mm) | $0.19 \pm 0.020$ |
| Mean cell angle, θ (deg) | $28 \pm 3$ |

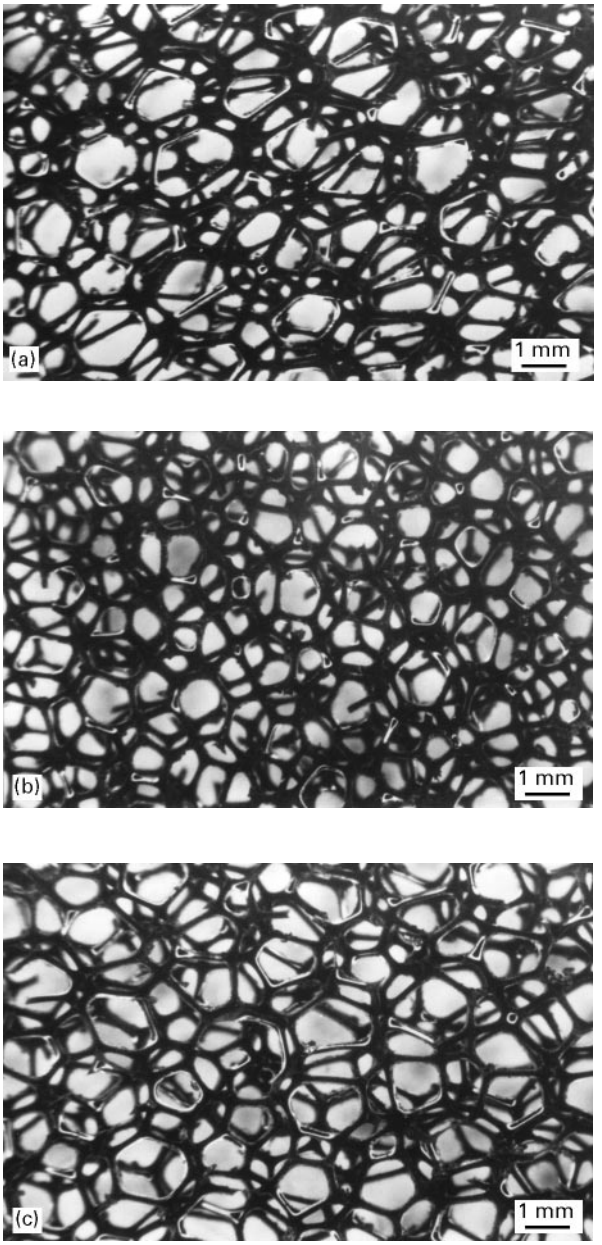


*Figure 3* Optical micrograph showing the microstructure of the 60 p.p.i. reticulated conventional polyester urethane foam (PECO): (a) looking at the foam along the $z$ axis (face B), (b) looking at the foam along the $y$ axis, foam rise direction (face C), (c) looking at the foam along the $x$ axis (face A).

Fig. 4 shows the microstructure of the 60 p.p.i. closed-cell conventional polyester urethane foam. In this closed-cell foam, most of the cell faces are closed off by thin membranes. The solid is not uniformly distributed between the edges and faces. The reason why the membranes are thinner than the cell ribs, is because during foaming surface tension draws solid into the cell edges. Descriptions of the foaming process can be found in Suh and Skochdopole [9].

Fig. 5(a–c) show the microstructures of 10, 30 and 60 p.p.i. open-cell conventional polyether urethane foams. Although a few of the cell membranes are perfect, most of the membranes are ruptured, so the gases are not trapped inside the cells, and the porous open-cell foams allow free movement of air throughout the materials when flexed. As a result, they are classified as open-cell foams. These foams with different cell sizes as shown in Fig. 5(a–c) are made from the same type of solid material (Polyether urethane). However, they have various cell geometry parameters (e.g., cell rib thickness etc.). Fig. 6 shows that the cell ribs have the conventional triangular cross-section formed during bubble expansion. The joining of two

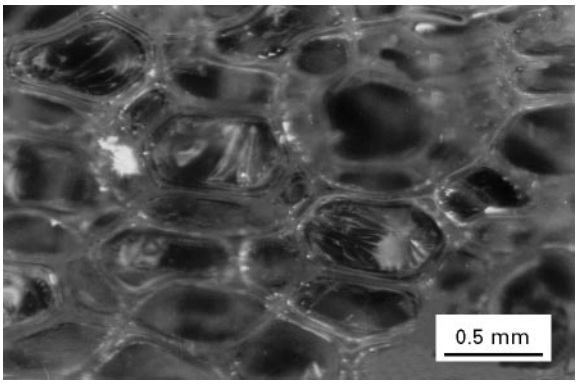


*Figure 4* Optical micrograph showing the microstructure of the 60 p.p.i. closed-cell conventional polyester urethane foam (PECC). Looking at the foam along the $z$ axis (face B).

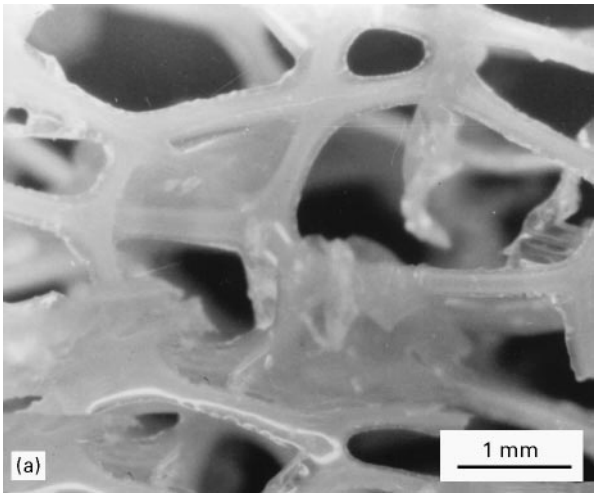


*Figure 5* Scanning electron micrograph showing the microstructure of the open-cell conventional polyether urethane foam, (a) looking at the 10 p.p.i. foam (10CO) along the $z$ axis (face B), (b) looking at the 30 p.p.i. foam (30CO) along the $z$ axis (face B) and (c) looking at the 60 p.p.i. foam (60CO) along the $z$ axis (face B).

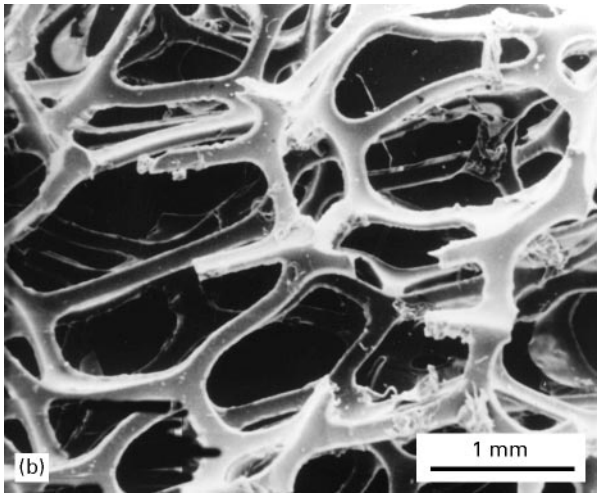


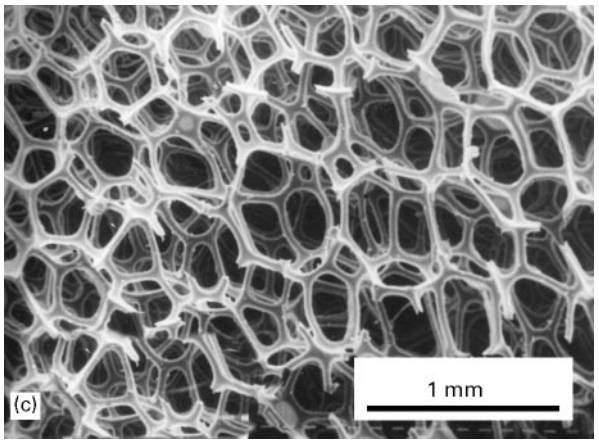


*Figure 5* (Continued).

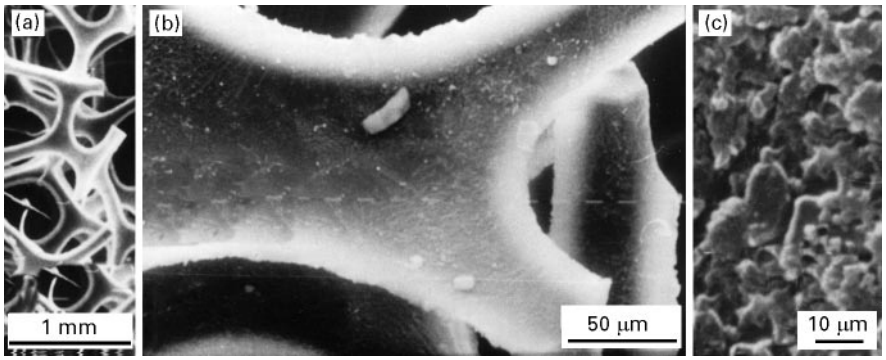


*Figure 6* The cell rib of the 60 p.p.i. closed-cell polyester urethane foam (PECC); (a) SEM × 30, (b) SEM × 220, (c) SEM × 3500.

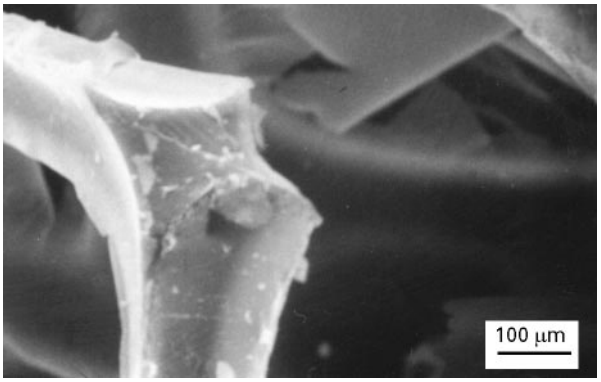


*Figure 7* SEM micrograph of the joint of the cell ribs of the 60 p.p.i. closed-cell polyester urethane foam (PECC).

ribs can be seen from Fig. 7 to be made of two triangles. The rib sections have uniform dimensions over a considerable proportion of their length, between the rib junctions.

From observation of the micrographs of these foams the following is worth stressing: (i) One important point to note here is that there is a wide variety of cell morphology within a foam specimen. For example, four and six sided faces are observed alongside the pentagonal faces. (ii) All the foams in this investigation are to some degree elongated, this is because of the way in which they are made. (iii) Apart from anisotropy, another important issue is the range of cell sizes in the foam. The average cell width in the foam rise direction is smaller than that in the other two directions, and there are a significant proportion of cells that are so small that they will not deform and therefore act as junction points within the foam.

## 3.2. The microstructure of auxetic foams

Micrographs of examples of auxetic foams are shown in Fig. 8(a–c). Fig. 8a is the 60 p.p.i. open cell polyether urethane foam whilst Fig. 8b is the 60 p.p.i. closed-cell polyether urethane foam, and Fig. 8c is the 30 p.p.i. open cell polyether urethane foam.

Using the methods described in Section 2 the geometric parameters listed in Tables VI–VIII were measured.

In the auxetic foams almost all the membranes of the closed-cell foams are ruptured due to the fabrication process. The auxetic foams have a re-entrant shape, but not all of the foam cells can be converted into the re-entrant shape. In particular the small cells remain unaffected by processing. During the fabrication process, most of the cell ribs have buckled, and some were broken; this is related to the increase in density compared to the parent conventional foam.

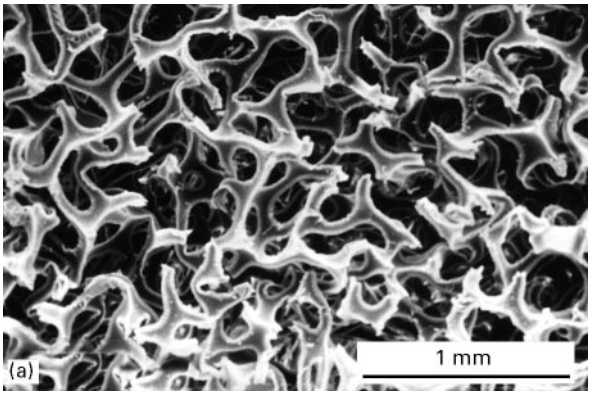


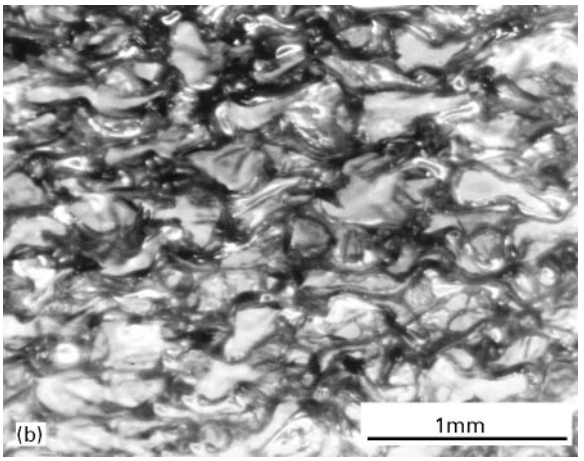


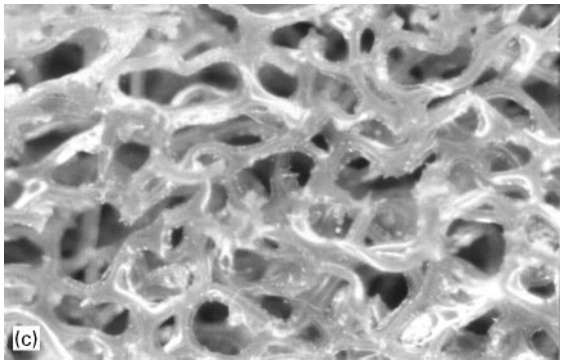


*Figure 8* Micrographs of the auxetic foams (a) the 60 p.p.i. open cell polyether urethane foam (60AO) (SEM) (b) the 60 p.p.i. closed-cell polyester urethane foam (PEAC) (optical microscopy) and (c) the 30 p.p.i. open-cell polyether urethane foam (30AO) (optical microscopy).

TABLE VI Characterization data for the 60 p.p.i. open cell polyether urethane auxetic foam (short hand: 60CO). (The volume of the auxetic foam is: $25.4 \times 25.4 \times 80$ mm, and the volume of its parent conventional foam is: $38 \times 38 \times 110$ mm)

| Material | Flexible polyether urethane (60AO) |
|---|---|
| Density, $\rho$ (kg m$^{-3}$) | $91 \pm 2.1$ |
| Open or closed cells | Reticulated |
| Mean edges per face | $6 \pm 2$ |
| Mean cell edge thickness, $t$ (mm) | $0.036 \pm 0.002$ |
| Average height of cell, $H$ (mm) | $0.285 \pm 0.08$ |
| Average waist height of cell, $W$ (mm) | $0.1 \pm 0.03$ |
| Rib length along the foam rise direction, $h$ (mm) | $0.38 \pm 0.04$ |
| Rib length along the other directions, $L$ (mm) | $0.19 \pm 0.05$ |
| Cell angle, $\theta$ (deg) | $-30 \pm 2$ |

TABLE VII Characterization data for the 60 p.p.i. closed-cell polyester urethane auxetic foam (short hand: PEAC). (The volume of the auxetic foam is: $25.4 \times 25.4 \times 80$ mm, and the volume of its parent conventional foam is: $38 \times 38 \times 110$ mm)

| Material | Flexible polyester urethane (PECA) |
|---|---|
| Density, $\rho$ (kg m$^{-3}$) | $72.4 \pm 2.5$ |
| Open or closed cells | Membranes are ruptured |
| Mean edges per face | $6 \pm 2$ |
| Mean cell edge thickness, $t$ (mm) | $0.045 \pm 0.015$ |
| Average height of cell, $H$ (mm) | $0.53 \pm 0.19$ |
| Average waist height of cell, $W$ (mm) | $0.24 \pm 0.09$ |
| Rib length along the foam rise direction, $h$ (mm) | $0.67 \pm 0.31$ |
| Rib length along the other directions, $L$ (mm) | $0.27 \pm 0.136$ |
| Mean cell angle, $\theta$ (deg) | $-32 \pm 3$ |

TABLE VIII Characterization data for the 30 p.p.i. open-cell polyether urethane auxetic foam (short hand: 100AO)

| Material | Flexible polyether urethane |
|---|---|
| Density, $\rho$ (kg m$^{-3}$) | $95 \pm 1.8$ |
| Open or closed cells | Open cells |
| Mean edges per face | $6 \pm 2$ |
| Mean cell edge thickness, $t$ (mm) | $0.11 \pm 0.045$ |
| Average height of cell, $H$ (mm) | $1.45 \pm 0.3$ |
| Average waist height of cell, $W$ (mm) | $0.76 \pm 0.06$ |
| Rib length along the foam rise direction, $h$ (mm) | $1.80 \pm 0.049$ |
| Rib length along the other directions, $L$ (mm) | $0.87 \pm 0.4$ |
| Mean cell angle, $\theta$ (deg) | $-24 \pm 3$ |

## 3.3. The microstructure of the cell ribs due to thinning

The cell rib thickness after thinning by the NaOH solution was measured from the SEM micrographs. The three pairs of photographs shown in Fig. 9(a–f) are typical of the thinning process. Further photographs were obtained and measured in order to obtain the data for the cell rib thickness versus the thinning time plotted in Fig. 10. It shows that the cell rib thickness is a function of the thinning time while the rib length remains constant. The thinning process is affected by: (i) the concentration of NaOH, (ii) thinning time, (iii) the thinning temperature, and (iv) the material of the cell ribs. To examine this effect on the mechanical properties of the foam the tensile modulus was measured, and the average values were used to plot Fig. 11.

## 3.4. Microscopic examination of foam deformation

### *3.4.1. Conventional foams under deformation*

Under tensile loading, the cells identified in Fig. 12(a–c) can be seen to be deforming. The ribs can be seen to be undergoing a combination of stretching, hinging and flexing. Eventually failure occurs by tensile fracture of highly stressed ribs.

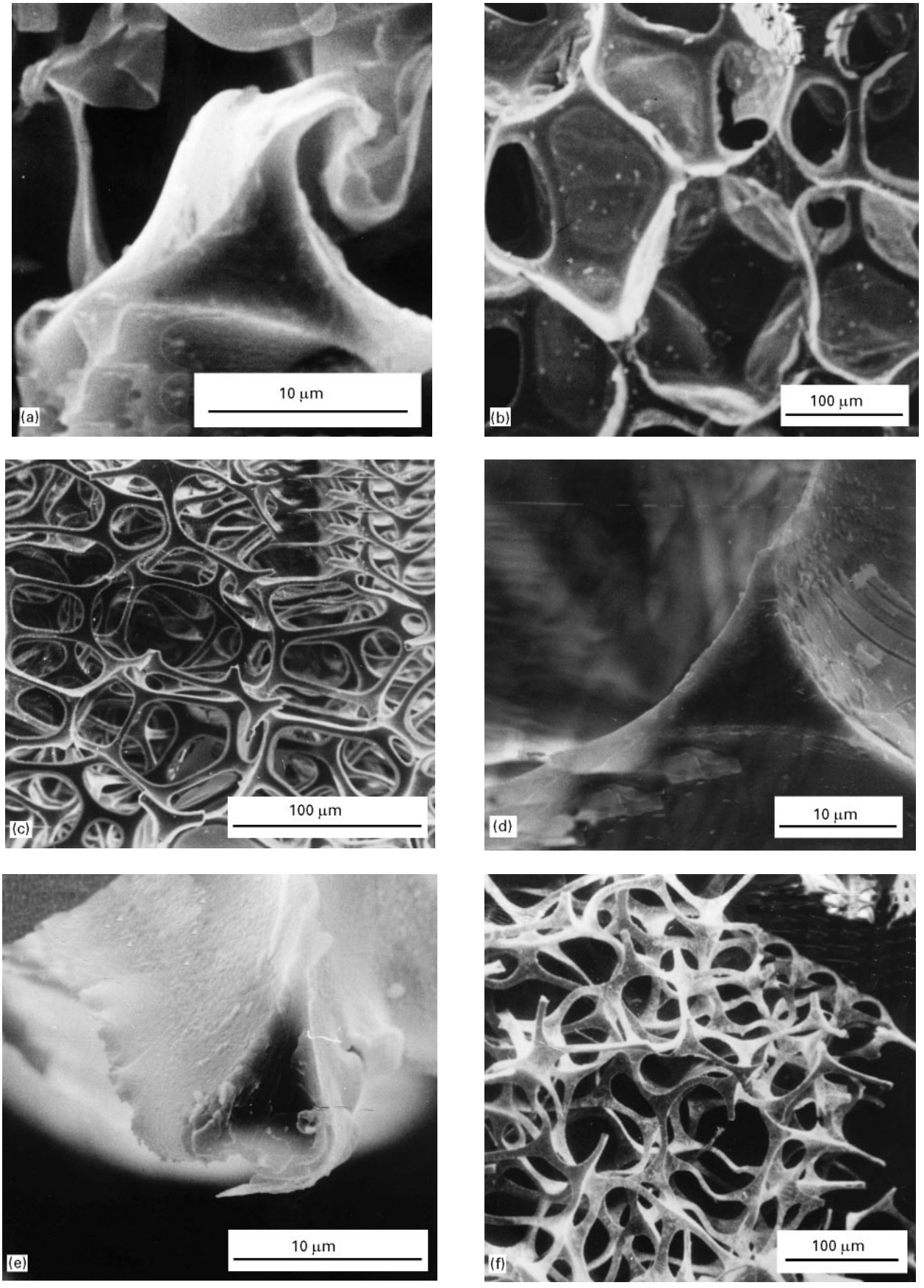


*Figure 9* The effects of the thinning process on the 60 p.p.i. closed-cell polyester urethane foam (PECC), (a) conventional, as received foam, magnification × 1250, (b) as (a) magnification × 40, (c) thinning for 20 min, magnification × 40, (d) as (c) magnification × 1250, (e) thinning for 50 mins, magnification × 1250 and (f) as (e), magnification × 40.

For compressive loading (see Fig. 13(a–f)), the stressing of individual ribs is similar to the case of tensile loading but of opposite sign. Flexure is the dominant mechanism, followed by buckling at high strains. Ribs perpendicular to the loading direction undergo deformation mainly by flexure.

Under shear loading (see Fig. 14(a–e)), the rib may be subjected to normal, bending or hinging stresses or

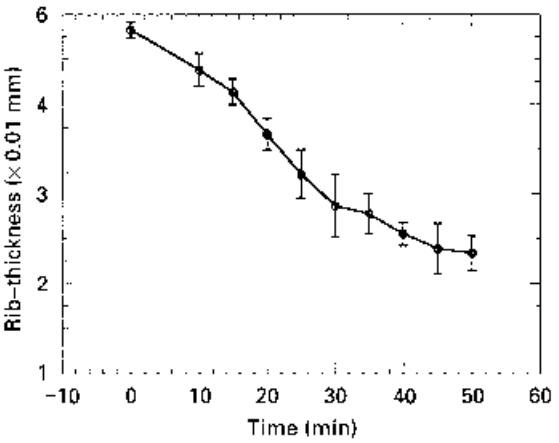


*Figure 10* A plot of the cell rib thickness as a function of thinning time for the 60 p.p.i. closed-cell polyester urethane foam (PECC).

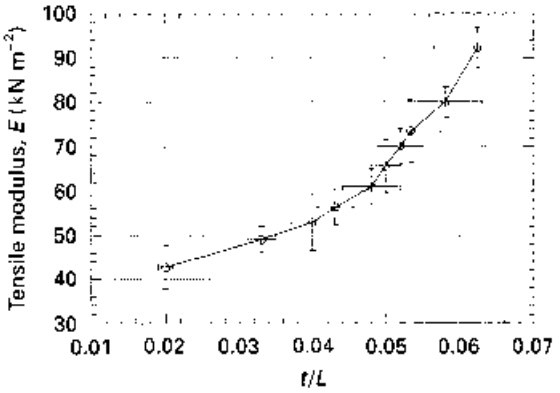


*Figure 11* Plot of tensile modulus, $E$, versus (cell rib thickness/cell rib length, $t/L$) for the 60 p.p.i. conventional closed-cell polyester urethane foam (PECC).

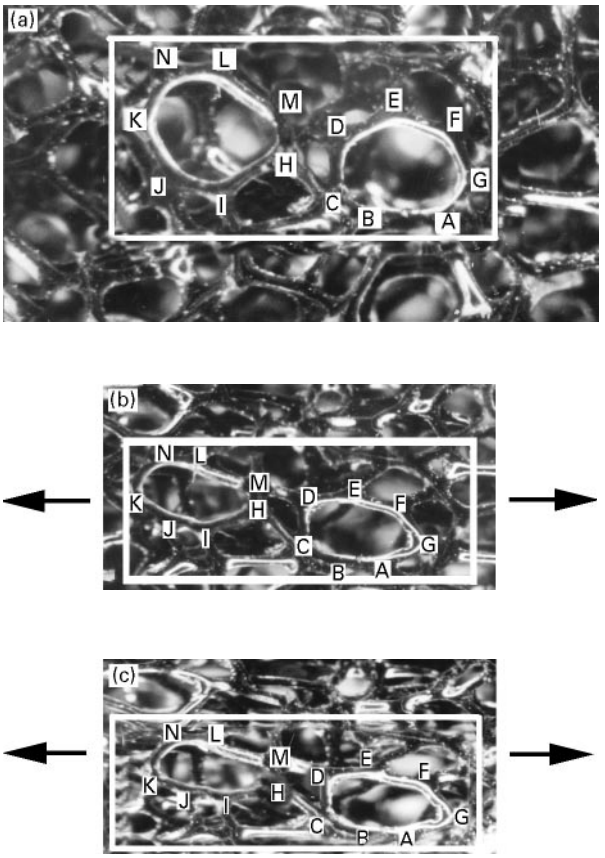


*Figure 12* The micrographs of the elastic tensile deformation of the 60 p.p.i. reticulated conventional polyester urethane foam (PECO) (note: looking at the foam along the $y$ axis). Stretching, hinging and flexing of the cell ribs can be seen. The tensile strains are: (a) $\varepsilon_x = 0$, (b) $\varepsilon_x = 12\%$ and (c) $\varepsilon_x = 25\%$.

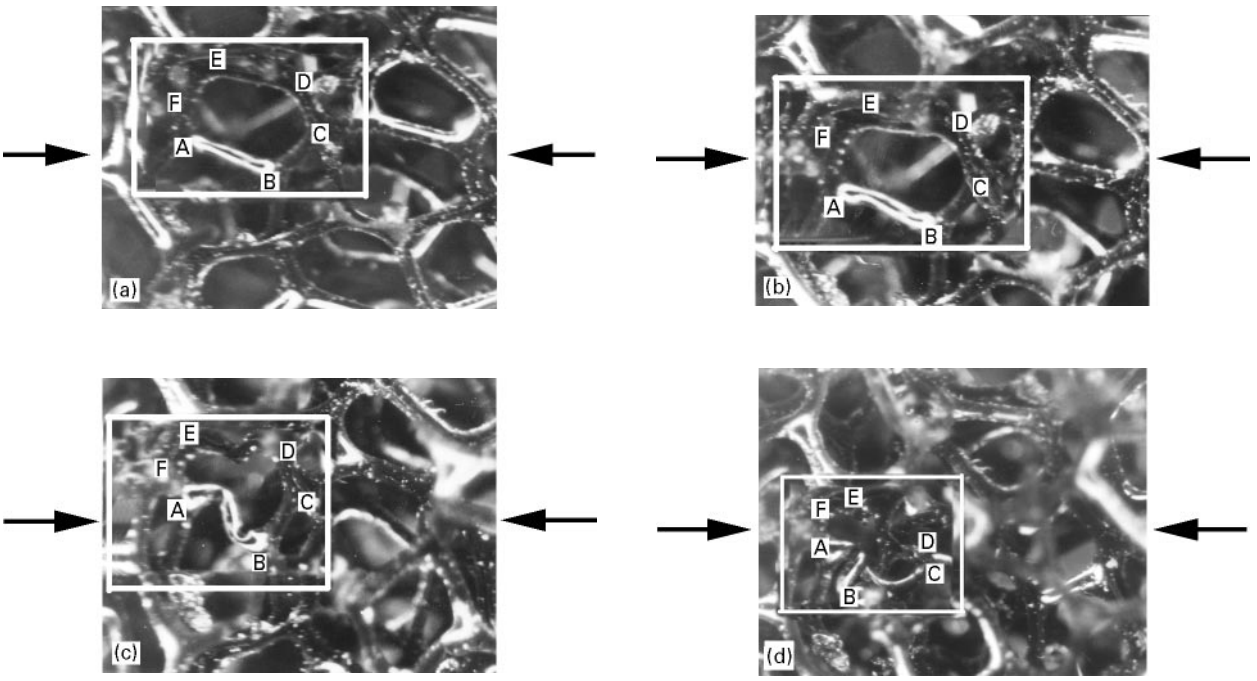


*Figure 13* Micrographs of the elastic compressive deformation of the 60 p.p.i. reticulated conventional polyester urethane foam (PECO) (note: looking at the foam along the $y$ axis). The compressive strains are: (a) $\varepsilon_y = 0\%$, (b) $\varepsilon_y = 3\%$ (cell ribs bending), (c) $\varepsilon_y = 10\%$ (cell rib buckling), (d) $\varepsilon_y = 20\%$ (cell rib collapse), (e) $\varepsilon_y = 40\%$ (elastic densification occurs), (f) $\varepsilon_y = 0\%$ (restored to its original shape). Note: the load axis is the same as the tension but is of the opposite sign.

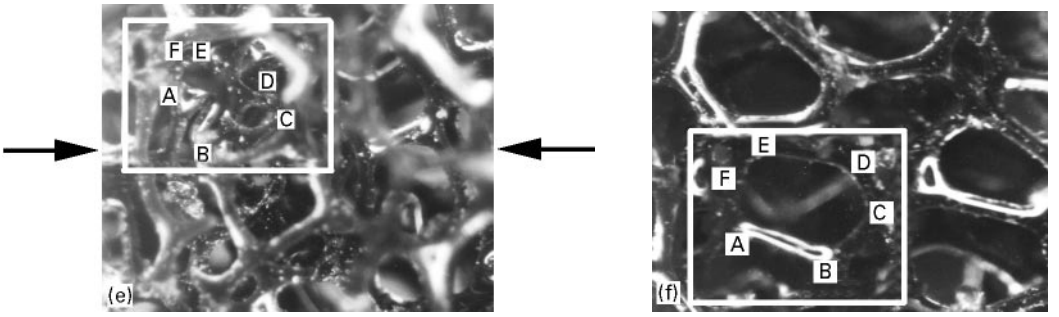


*Figure 13* (Continued).

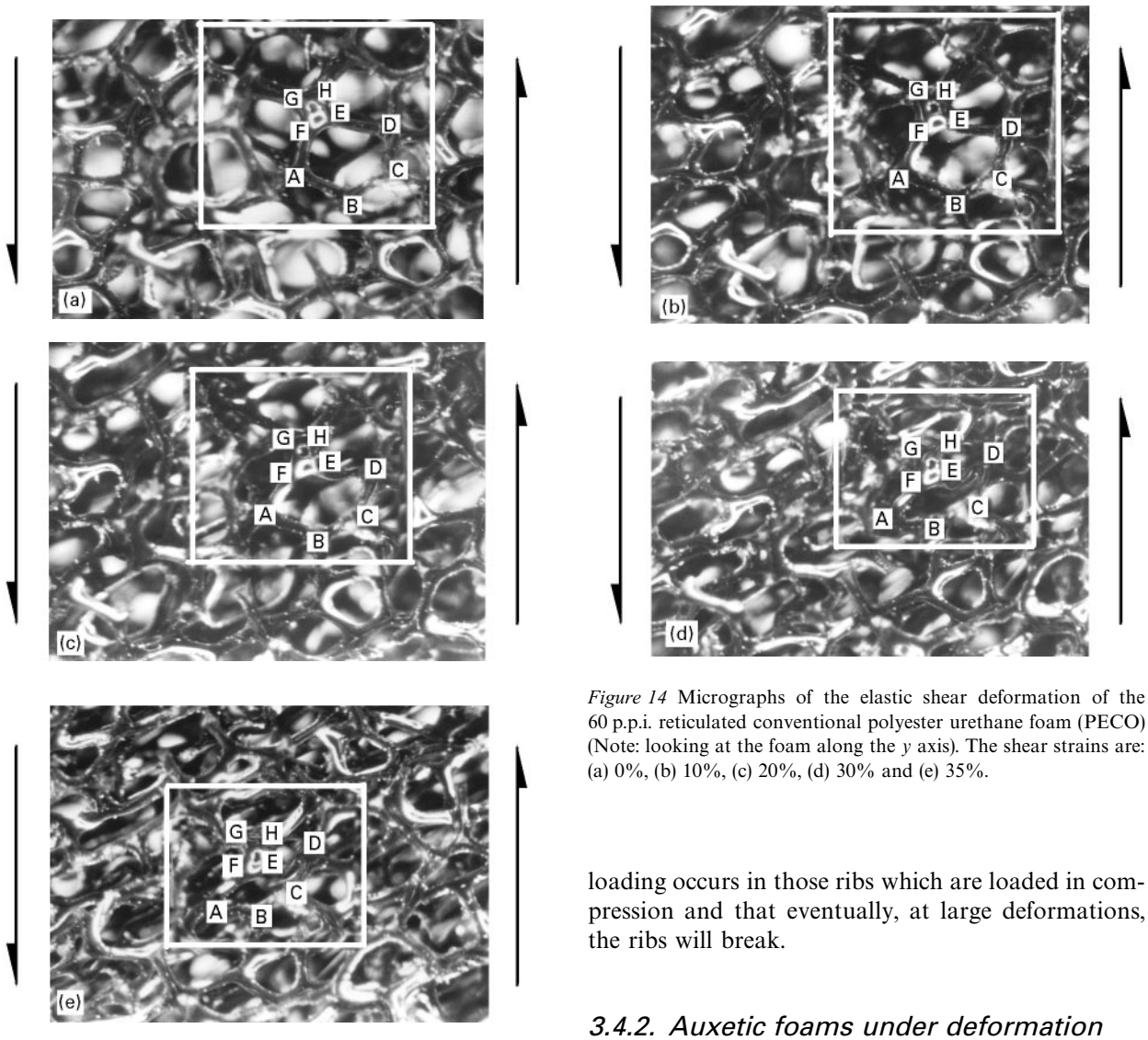


*Figure 14* Micrographs of the elastic shear deformation of the 60 p.p.i. reticulated conventional polyester urethane foam (PECO) (Note: looking at the foam along the *y* axis). The shear strains are: (a) 0%, (b) 10%, (c) 20%, (d) 30% and (e) 35%.

a combination of the three. In this case the critical stresses for non-linear foam deformation is therefore due to a combination of stretching, hinging and buckling. Failure occurs due to buckling of those ribs that lie at an angle of about 45° to the direction of the external load. At higher loads, rib fracture starts to occur. Fig. 14(a–e) shows a shear loaded conventional foam at different stages of deformation. It can clearly be seen that the very thin cell ribs buckle and wrinkle under small deformation. The cell in the white frame rotates anti-clockwise. The deformation under shear loading occurs in those ribs which are loaded in compression and that eventually, at large deformations, the ribs will break.

### 3.4.2. Auxetic foams under deformation

Auxetic foams have a more complex, re-entrant geometry (Fig. 15a). They are, therefore much more likely to deform by hinging and flexure rather than stretching in both tension (Fig. 15b) and compression (Fig. 15c). Under tension (Fig. 15b) the cells are seen to expand transversely under a longitudinal tensile force.

Fig. 15(a–c) show that the deformation mechanism of an auxetic foam is the same as that for a conventional foam. However, because an auxetic foam cell has a dumb-bell like cell shape, it becomes thinner in the transverse direction in compression, and becomes fatter in tension. A conventional foam cell with a convex cell shape expands in the transverse direction under compression, but shrinks under tension. In this

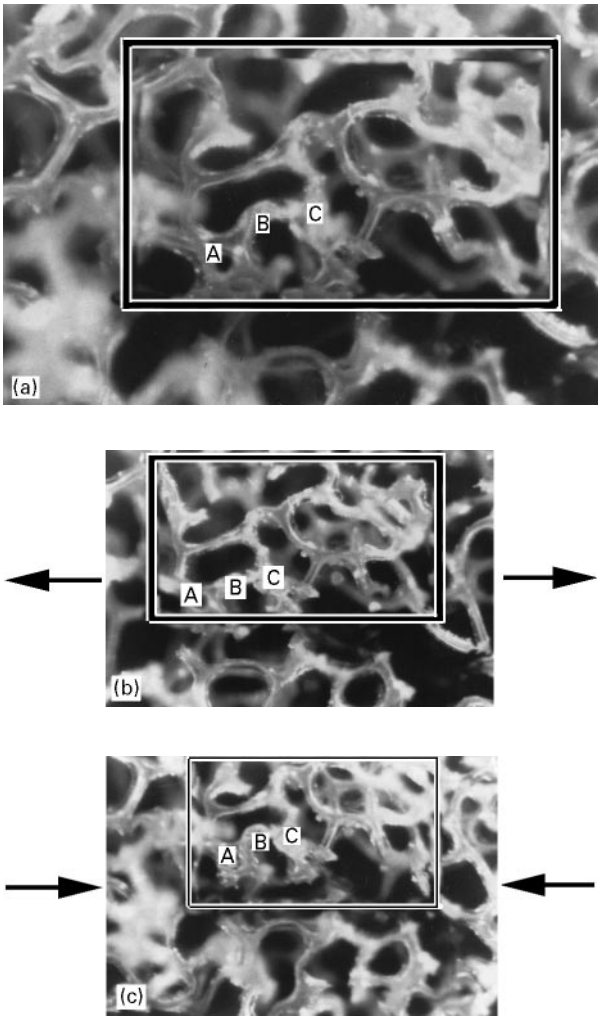


*Figure 15* Micrographs showing the elastic deformation of the 60 p.p.i. reticulated auxetic polyester polyurethane foam (PEAO); (a) unloaded, (b) under tension and (c) under compression.

investigation, the specimens are elastic materials, and can therefore recover from their deformations after the deforming forces have been removed.

Fig. 16(a–d) shows a shear loaded auxetic foam at different stages of deformation. The series of illustrations show the possible deformation modes, i.e., bending, stretching, hinging, and indicate clearly that rotation does occur.

## 4. Discussion

An attempt was made to analyse the effect of thinning on the Young's modulus (Fig. 17) using the model of Gibson and Ashby [8]:

$$\frac{E}{E_s} = k\left(\frac{\rho}{\rho_s}\right)^2 \tag{13}$$

where $E$ is the Young's modulus of foam, $E_s$ is the Young's modulus of solid flexible polyurethane, $\rho$ is density of the foam, $\rho_s$ is the density of solid flexible polyurethane and $k$ is a constant. The normalizing properties $\rho_s = 1.2\ \mathrm{Mg\,m^{-3}}$ and $E_s = 45\,000\ \mathrm{kN\,m^{-2}}$ for the flexible polyurethane foams are chosen from Gibson and Ashby [8]. In Fig. 17, the experimental data are plotted as symbols. For high densities the experimental and theoretical results are in good agreement. However as the density decreases due to thinning, the modulus does not decrease as rapidly as would be expected from a simple flexure model.

An extra analysis plot using $\log E$ versus $\log(L/t)$ to investigate any possible power law dependence from the gradient is shown in Fig. 18. It shows that $\log E$ is almost linear to $\log(L/t)$ when the cell

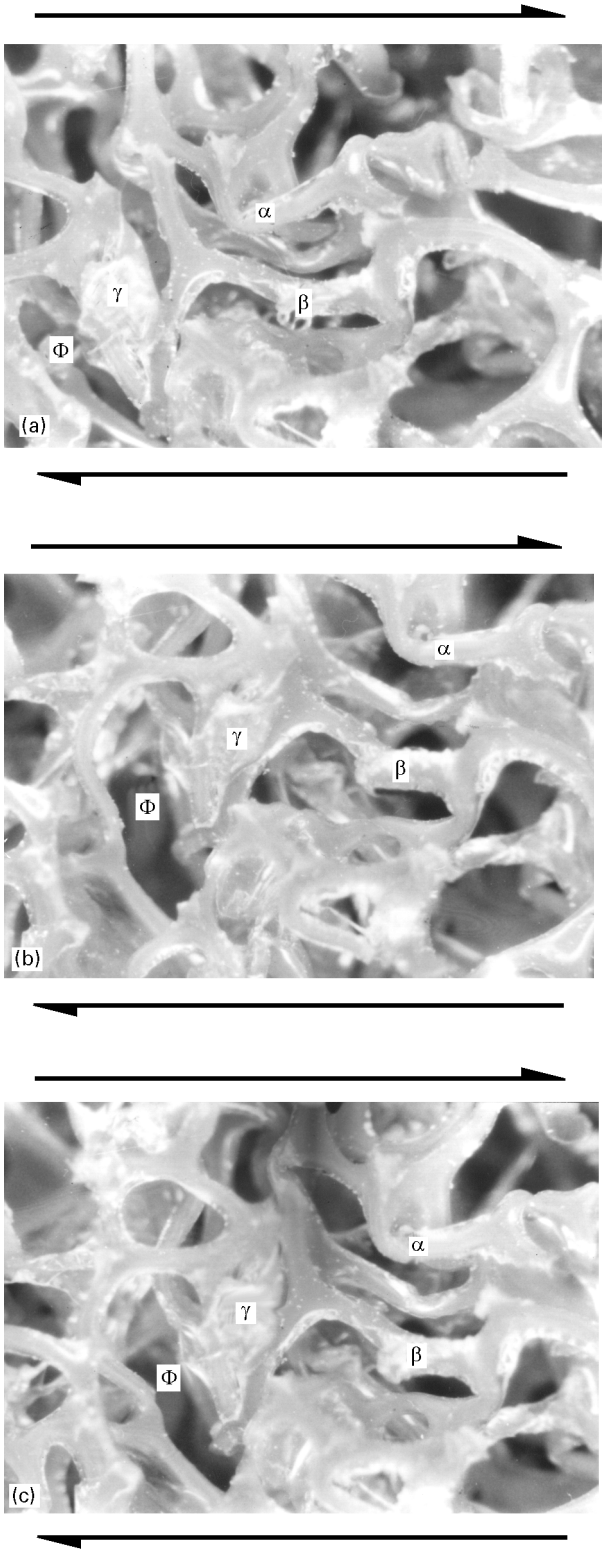


*Figure 16* Micrographs of the elastic deformation of the 10 p.p.i. reticulated auxetic polyether polyurethane foam (70AO). The shear strains are: (a) 0%, (b) 10%, (c) 20% and (d) 30%.

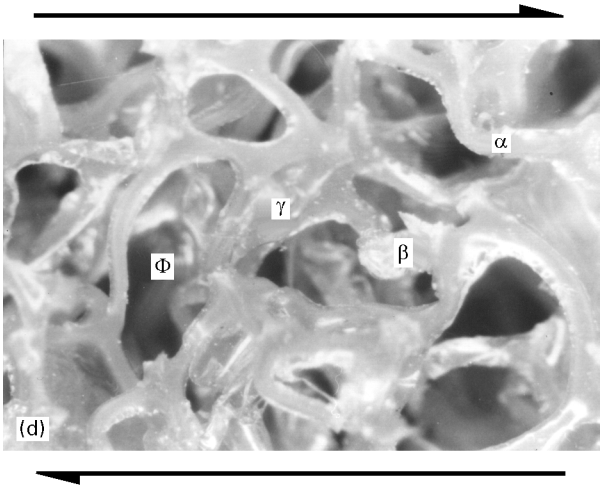


*Figure 16* (Continued).

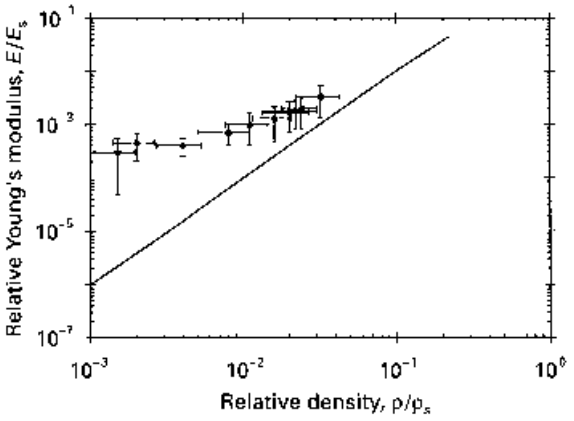


*Figure 17* Data for the relative Young's modulus of the foams, $E_y/E_s$, plotted against relative density, $\rho^*/\rho_s$. The solid line represents the theory of Gibson and Ashby [8].

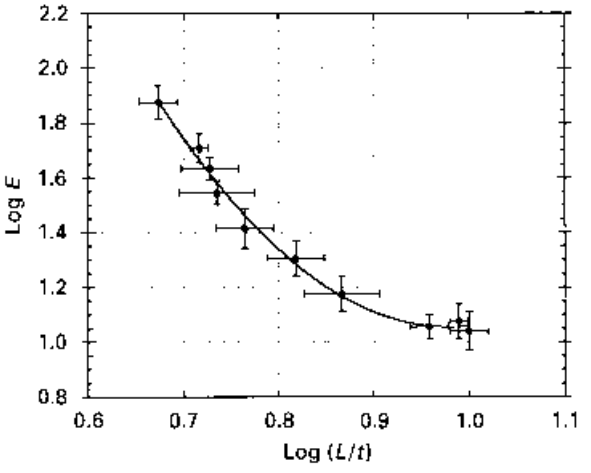


*Figure 18* Plot of $\log E$ versus $\log(L/t)$ for the 60 p.p.i. closed-cell polyester urethane foam (PECC). ($E$ is the tensile modulus, $L$ is the cell rib length, and $t$ is the cell rib thickness of foam PECC).

rib thickness is greatest. However, when the cell rib is thinned down to very fine values then the chemical composition and the shape of cells may be changed, and cell ribs begin to break.

From the analysis of Gibson and Ashby $E \propto t^4$ if the predominant mechanism is flexure while $E \propto t^2$ for stretching [8]. From Fig. 18 it can be seen that the data are close to $E \propto t^4$ for large $t$ values but the power law diminishes for lower $t$ values. This indicates that stretching becomes more important as the foam is thinned.

## 5. Conclusion

From the above it may be concluded that a simple tetrakaidecahedral model is not sufficient to cope with anisotropic foams demonstrating a preferential rise direction. A simple geometry has been developed that can cope both with anisotropy and the conversion to a re-entrant form, as exhibited by auxetic foams. The relevant geometric parameters have been measured. These parameters are used in a model for the mechanical properties of the foams described elsewhere [10].

The microstructural deformation of auxetic foams have been examined and the mechanism causing auxetic behaviour has been observed. Although rib flexure has been described as being the dominant mechanism for foam deformation [8], evidence for the occurrence of rib stretching is also presented here. This is confirmed when the ribs are thinned and comparison with the expected dependence of $E$ on $t$ examined.

In general, flexure dominates in auxetic foams and in conventional foams in compression. Whereas stretching is observed, together with flexure, in conventional foams under tension.

## Acknowledgements

Dr. N. Chan would like to thank the Department of Materials Science and Engineering, University of Liverpool, for the provision of departmental facilities during her PhD study.

## References

1. R. S. LAKES, *Science* **235** (1987) 1038.
2. A. E. H. LOVE, *Phil. Trans.* **10** (1891) 393.
3. R. S. LAKES, *Adv. Mater.* **5** (1993) 293.
4. B. D. CADDOCK and K. E. EVANS, *J. Phys.* **D22** (1989) 1870.
5. K. L. ALDERSON and K. E. EVANS, *Polym.* **33** (1992) 4435.
6. A. P. PICKLES, K. L. ALDERSON and K. E. EVANS, *Polym. Engng Sci.* **36** (1996) 636.
7. K. E. EVANS, M. A. NKANSAH, I. J. HUTCHINSON and S. C. ROGERS, *Nature* **353** (1991) 124.
8. L. J. GIBSON and M. F. ASHBY, "Cellular solids: structure and properties", (Pergamon Press, London, 1988).
9. K. W. SUH and R. E. SKOCHDOPOLE, in "Encyclopedia of chemical technology", Vol. 2, edited by M. Grayson, 3rd Edn (Wiley, New York, 1980) p. 82.
10. N. CHAN, PhD thesis, University of Liverpool (1995).
11. N. CHAN and K. E. EVANS, *J. Mater. Sci.* **32** (1997).
12. A. N. GENT and A. G. THOMAS, *J. Appl. Polym. Sci.* **1** (1959) 107.

*Received 17th June 1996*
*and accepted 1st May 1997*